

Highly efficient iridium(III) complexes with diphenylquinoline ligands for organic light-emitting diodes: Synthesis and effect of fluorinated substitutes on electrochemistry, photophysics and electroluminescence

Xiaowei Zhang^a, Jia Gao^b, Chuluo Yang^{a,*}, Linna Zhu^a, Zhongan Li^a,
Kai Zhang^a, Jingui Qin^a, Han You^b, Dongge Ma^{b,*}

^a Department of Chemistry, Hubei Key Lab on Organic and Polymeric Optoelectronic Materials, Wuhan University, Wuhan 430072, China

^b State Key Laboratory of Polymer Physics and Chemistry, Changchun Institute of Applied Chemistry, Chinese Academy of Sciences, Changchun 130022, China

Received 4 May 2006; received in revised form 22 June 2006; accepted 7 July 2006

Available online 18 July 2006

Abstract

A series of novel cyclometalated iridium(III) complexes bearing 2,4-diphenylquinoline ligands with fluorinated substituent were prepared and characterized by elemental analysis, NMR and mass spectroscopy. The cyclic voltammetry, absorption, emission and electroluminescent properties of these complexes were systematically investigated. Electrochemical studies showed that the oxidation of the fluorinated complexes occurred at more positive potentials (in the range 0.57–0.69 V) than the unfluorinated complex **1** (0.42 V). In view of the energy level, the lowering of the LUMO by fluorination is significantly less than that of the HOMO. The weak and low energies absorption bands in the range of 300–600 nm are well resolved, likely associated with MLCT and $^3\pi-\pi^*$ transitions. These complexes show strong orange red emission both in the solution and solid state. The emission maxima of the fluorinated complexes showed blue shift by 9, 24 and 15 nm for **2**, **3** and **4**, respectively, with respect to the unfluorinated analogous **1**. Multilayered organic light-emitting diodes (OLEDs) were fabricated by using the complexes as dopant materials. Significantly higher performance and lower turn-on voltage were achieved using the fluorinated complexes as the emitter than that using the unfluorinated counterpart **1** under the same doping level. OLED devices using complexes **2** and **3** as the phosphorescent dopant at 3 wt% doping level exhibit very high performance. To complex **2**, the maximum luminance is 16410 cd/m² at a current density of 210 mA/cm², and the maximum luminance efficiency and power efficiency are 9.34 cd/A and 5.20 lm/W, respectively, with the emission of 605 nm. To complex **3**, those data are 16797 cd/m² at a current density of 211 mA/cm², 11.12 cd/A and 4.97 lm/W, respectively, with the emission of 593 nm.

© 2006 Elsevier B.V. All rights reserved.

Keywords: Iridium complexes; Phenylquinoline; Fluorination; Electrochemistry; Photophysics; Electroluminescence

1. Introduction

Recently, the iridium complexes as phosphorescent emitter in organic light-emitting diodes (OLEDs) have attracted much attention since the realization of a high efficiency OLED device based on the complex *fac*-tris(2-phenylpyridine)iridium [Ir(ppy)₃] [1]. The frequency of emission of the iridium complexes can usually be tuned by modification or variation of cyclometalated ligands of 2-phenylpyridine or its analogical ligands, such as benzoisoquinolines [2], 2-phenylbenzothiazole [3], benzoimidazole [4], etc. Several groups have studied the mechanism of the OLEDs based on phosphorescent heavy metal complexes [5]. It has been demonstrated that the Förster energy transfer plays minor role in achieving high efficiency in

* Corresponding authors. Tel./fax: +86 27 68756757.

E-mail address: clyang@whu.edu.cn (C. Yang).

these devices, instead that direct charge trapping plays dominant role in electroluminescence. Therefore, in order to obtain high efficiency OLED devices, it would be desirable to design the phosphorescent complexes as energy acceptors, more importantly, as traps for holes or/and electrons.

Quinoline-based compounds have received considerable attention in optoelectronic materials due to their high electron affinities. For example, aluminum tris(8-hydroxyquinolate) (AlQ₃) has been usually applied as electron transporting, electron-emitting and host materials in doped OLED systems. Most recently, phenylquinoline or phenylisoquinoline based iridium complexes have been proven to be good red emitters [2,6]. On the other hand, iridium complexes carrying fluorinated phenylpyridyl ligands have shown several benefits, such as enhancing the photoluminescence efficiency and improving the sublimation [7].

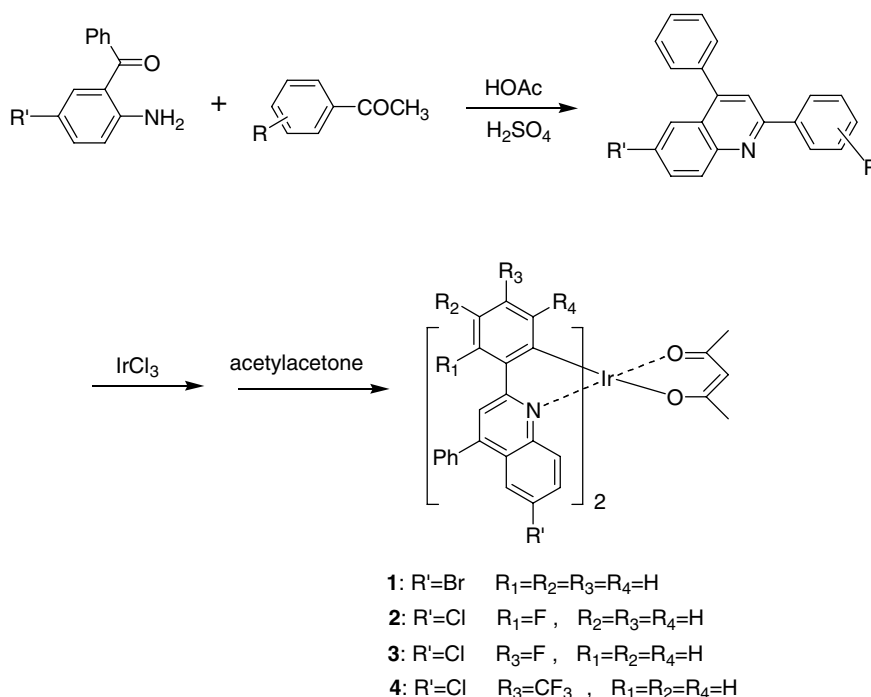
In this paper, we report a series of novel iridium complexes bearing 2,4-diphenylquinoline ligands with strong electron-withdrawing fluorinated substituent, as well as the unfluorinated analogue for comparison. We expect that the phenylquinoline ligands modified by fluorinated substituent could improve the electron transport ability of the complexes, consequently to facilitate the charge trapping across the bulk for high performance OLEDs [8]. Meanwhile, it will be significant to study the effect of fluorinated substituent on the electrochemistry, photophysics and electroluminescent performance of iridium complexes in order to understand the relationship between the structures and properties. In addition, the bulky phenyl group in the position 4 of quinoline ring may prevent the crystallization and

suppress the aggregation-forming tendency, and the chloride or bromide in the position 6 of quinoline ring may increase luminescent efficiency by heavy-atom effect.

2. Results and discussion

2.1. Synthesis and characterization

Phenylquinoline-based organic ligands were conveniently prepared from 5-chloro-2-aminobenzophenone (or 5-bromo-2-aminobenzophenone) and corresponding acetophenone derivatives through Friedländer reaction in moderate yields (Scheme 1) [9]. The Ir(III) μ -chloro-bridged dimers were synthesized by the reaction of iridium trichloride hydrate with ligands according to a conventional procedure [10]. Then the diiridium complexes were converted to mononuclear iridium complexes by replacing the two bridging chlorides with bidentate monoanionic acetylacetonate ligand in 50–70% yields. Elemental analysis of each of the four complexes is consistent with the expected formulation of their structures. The mass spectra give corresponding molecular ion peaks at 1010 for **1**, 956 for **2** and **3**, and 1056 for **4**. In the ¹H NMR, the acetylacetonate CH protons appear in the region 4.69–4.79 ppm as a sharp singlet, obviously lower than the corresponding signals usually appeared at >5.1 ppm in the other iridium complexes with arylpyridine ligands. This is presumably due to the weaker ligand field strength of quinoline that inhibits effective back-donation from metal center to ligand, consequently, metal center has larger electron density which more shields the acetylacetonate CH protons [6].



Scheme 1. Synthesis of the iridium complexes.

2.2. Electrochemistry

The electrochemical behaviors of the four complexes were examined by using cyclic voltammetry. The cathodic and anodic scans were carried out in THF and CH_2Cl_2 solution at 298 K, respectively (Fig. 1). The redox potentials, measured relative to an internal ferrocenium/ferrocene reference (Fc^+/Fc), are listed in Table 1.

The unfluorinated complex **1** shows three quasi-reversible reduction waves, whereas the fluorinated complexes exhibit two fully reversible reduction processes. The first and second reduction potentials of the complexes stay in a range of -1.99 to -2.12 V and -2.22 to -2.30 V, respectively. On the other hand, each of four complexes only displays a reversible one-electron oxidation couple. The oxidation of three fluorinated complexes occur at significant more positive potentials (in the range 0.57 – 0.69 V) than the unfluorinated complex **1** (0.42 V). These values are similar to the reported bis-cyclometalated iridium complexes [2,6,11]. As revealed previously by electrochemistry

and theoretical calculations of cyclometalated Ir(III) complexes, reduction is generally considered to mainly occurs on the heterocyclic portion of the cyclometalated $\text{C}^{\wedge}\text{N}$ ligands, whereas oxidation process largely involves the Ir–aryl center [12]. Consistent with this conclusion, the fluorinated substitutes of the 2-phenyl group have less affection on the reduction potentials, in contrast, they notably increase the oxidation potentials with respect to the unfluorinated complex. In view of the energy level, the fluorinated substitution leads to a larger decrease for the HOMO than the LUMO orbitals, in consequence resulting in a widening of the HOMO–LUMO gap, in comparison with the parent complex **1**.

On the basis of the onset potentials of the oxidation and reduction, the HOMO and LUMO energy levels of these iridium complexes with regard to the energy level of ferrocene (4.80 eV below vacuum) are estimated (Table 1) [13]. Both the HOMO and LUMO levels of the fluorinated complexes are lower than that of the parent complex **1**, respectively. If this trend remains the same in the solid state, the

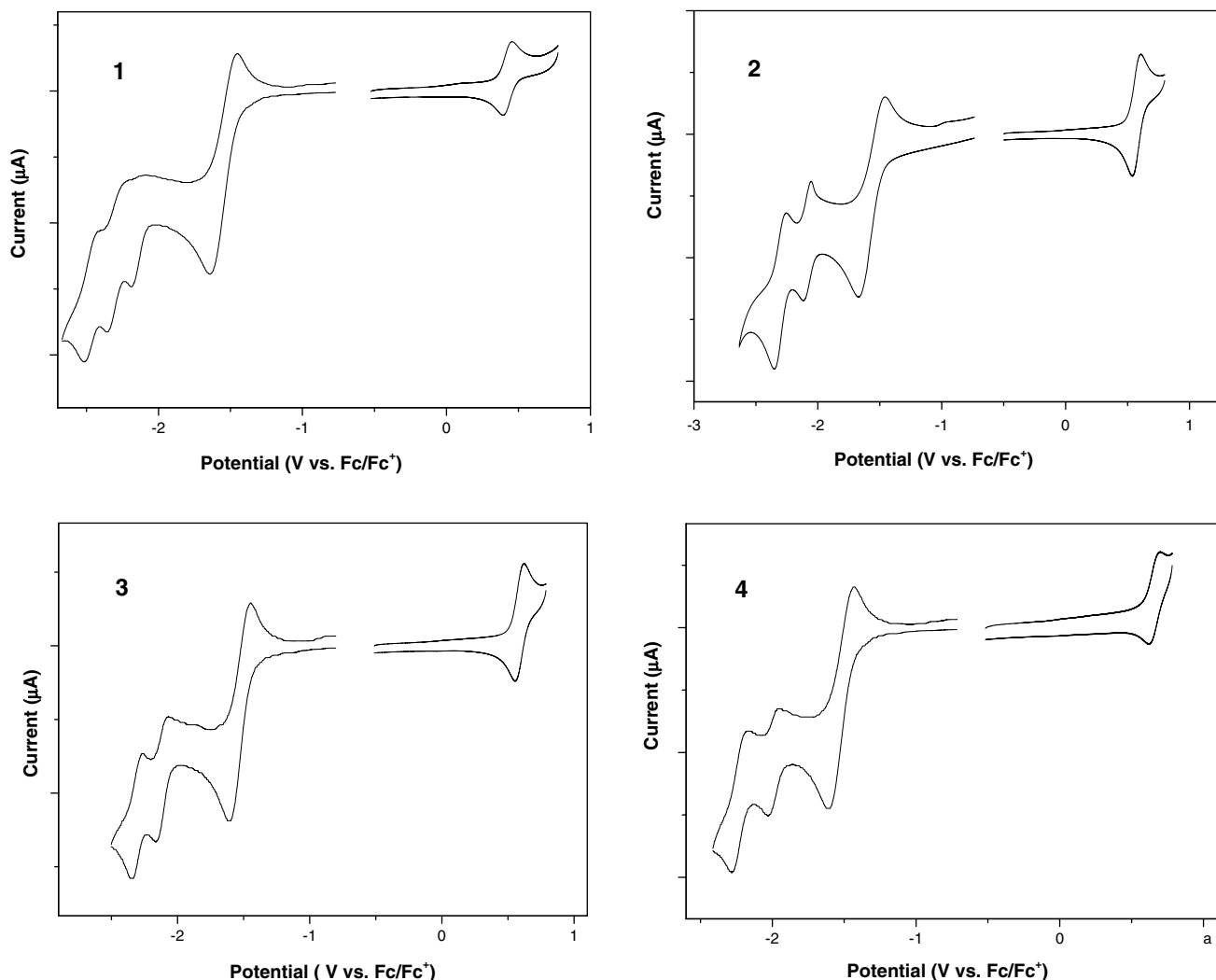


Fig. 1. Cyclic voltammograms of the four complexes (the first reduction couple come from the solvent THF).

Table 1
Electrochemical properties of the Ir complexes

Complex	$E_{1/2}^{\text{ox}}$ (V) ^a	$E_{1/2}^{\text{red}}$ (V) ^a	$E_{\text{onset}}^{\text{ox}}$ (V) ^a	$E_{\text{onset}}^{\text{red}}$ (V) ^a	HOMO (eV) ^b	LUMO (eV) ^c	E_{gap} (eV)
1	0.42	−2.46, −2.28, −2.14	0.35	−2.09	−5.15	−2.71	2.44
2	0.57	−2.30, −2.09	0.50	−2.00	−5.30	−2.80	2.50
3	0.59	−2.30, −2.12	0.52	−2.05	−5.32	−2.75	2.57
4	0.66	−2.22, −1.99	0.59	−1.93	−5.39	−2.87	2.52

^a Potential values are reported vs. Fc/Fc⁺.

^b Determined from the onset oxidation potential.

^c Determined from the onset reduction potential.

electron injection barrier for the fluorinated complexes will be less than their counterpart **1**. This will be discussed in Section 2.4.

The reversibility of the redox waves of the fluorinated iridium complexes suggests good stability of both their cations and anions, which is very beneficial to the long term stability of OLED devices fabricated from these materials.

2.3. Absorption and emission

Fig. 2 shows the absorption spectra of four complexes. Absorption peak wavelengths and the molar extinction coefficients are given in Table 2. Intense absorptions are observable in the ultraviolet region of the spectra, between 250 and 300 nm, which are attributed to transitions of ligand-centered states with mostly spin-allowed $^1\pi-\pi^*$ char-

acter from cyclometalated C^N ligands. Relatively weaker absorption bands in the range of 300–400 nm are well resolved, ascribing to a spin-allowed metal-to-ligand charge transfer ($^1\text{MLCT}$) transition. The long tail extended to lower energies (in the range of 400–600 nm) can be likely associated with both $^3\text{MLCT}$ and $^3\pi-\pi^*$ transitions, which gains considerable intensity by mixing with the $^1\text{MLCT}$ transition through the spin-orbit coupling [1f,14].

The emission spectra of **2**, **3** and **4** in dichloromethane show emission peak at 602, 587 and 596 nm, which blue shifted by 9, 24 and 15 nm, respectively, when compared with the unfluorinated counterpart **1** (Table 2 and Fig. 2 inset), falling in orange red region. The *meta* position on the 2-phenyl ring, with respect to the fluoride or trifluoromethyl substituent, is electron deficient, decreasing the σ donation from the cyclometalated ligand to iridium, and thus the HOMO levels mainly related to the Ir–aryl center lowered in comparison with the unfluorinated analogous **1**, which is supported by the fact that the oxidation potentials of **2–4** are significantly higher than that of **1**. This results in an energy increase of the $^3\text{MLCT}$ emitting level in the fluorinated complexes. The alteration of energy gap evaluated from the results of cyclic voltammetry (Table 1). It is noteworthy that the complex **3** with fluorine at the *meta* position 3, with respect to the coordination carbon, exhibits significantly larger hypsochromic shift (24 nm) than complex **2** (9 nm) with fluorine at the *meta* position 5, indicating the *meta* position 3 is more effective in tuning the emission towards the blue region than the *meta* position 5. To our knowledge, this is the first example to distinguish the effect of different *meta* fluorine substitution on emission of cyclometalated iridium complexes [15]. It is also interesting to note the complex **4** with trifluoromethyl substituent at the *meta* position to iridium exhibit bathochromic shift by 9 nm with respect to the analogue complex **3** with *meta*

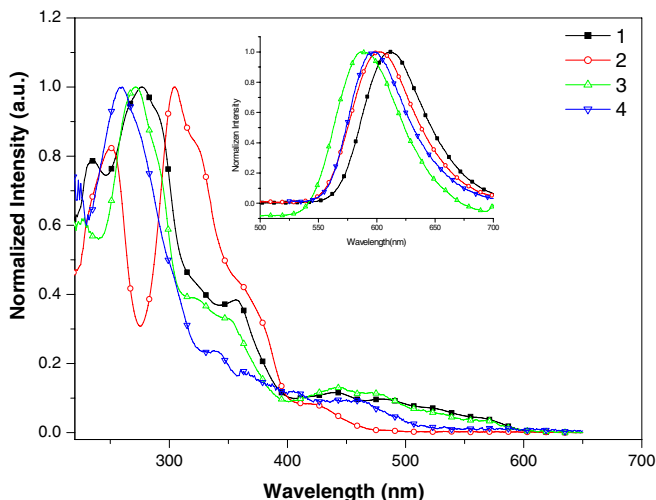


Fig. 2. Absorption and emission (inset) spectra of the complexes in CH₂Cl₂.

Table 2
Absorption and emission data for Ir complexes

Complex	Absorbance λ/nm ($\log \epsilon$) ^a	Emission λ_{max} (nm) ^a	Quantum yield ^{a,b}
1	277 (4.7), 356 (4.5), 440 (4.0), 479 (3.7)	611	0.28
2	250 (4.3), 304 (4.6), 352 (4.3), 417 (3.5)	602	0.34
3	272 (4.7), 350 (4.2), 447 (3.8), 474 (3.8)	587	0.32
4	260 (4.8), 339 (4.2), 361 (4.1), 403 (3.9), 459 (3.8)	596	0.25

^a Measured in CH₂Cl₂.

^b The relative quantum yields were calculated relative to Ir(ppy)₂(acac) ($\Phi_{\text{em}} = 0.34$).

fluorine substituent. This is contrary to the corresponding iridium complexes with fluorinated phenylpyridine ligand, where a hypsochromic shift was observed in the same situation [7a].

2.4. Electroluminescent properties

The four complexes show moderate to good triplet quantum efficiencies (Table 2). To illustrate the electroluminescent properties of these complexes, typical OLED devices using these complexes as dopants in the emitting layer have been fabricated (Fig. 3). All device consist of multilayer configurations ITO/NPB (40 nm)/CBP + 3–8% dopant (30 nm)/BCP (10 nm)/AlQ₃ (30 nm)/LiF(1 nm)/Al (100 nm), in which 4,4'-biscarbazolylbiphenyl (CBP) serves as host for iridium complexes, 2,9-dimethyl-4,7-diphenyl-1,10-phenanthroline (BCP) as hole and exciton blocker, and 4,4'-bis[*N*-(1-naphthyl)-*N*-phenylamino]biphenyl (NPD) and tris(8-hydroxyquinoline)aluminum (AlQ₃) as hole transporting and electron transporting materials, respectively [16].

All devices display intense orange-red or red emission in the range of 593–616 nm in the EL spectra, which resembled to those of the PL spectra in dichloromethane solution, indicating that the EL emissions of the device originate from the triplet excited states of the phosphors. Figs. 4 and 5 show the current–voltage curves and the luminance–current density characteristics of the devices, respectively. The current efficiency (η_c) as functions of current

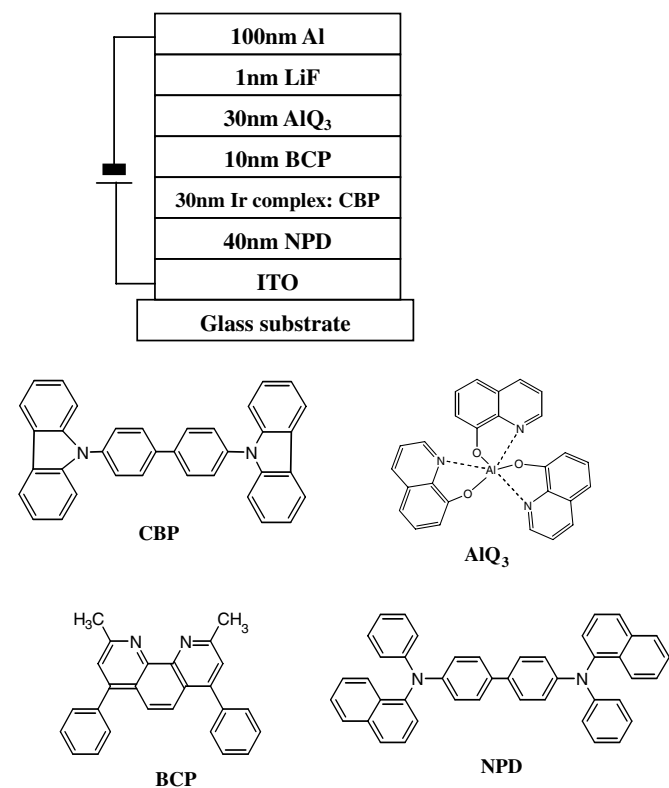


Fig. 3. Device configurations and molecular structures used in the devices.

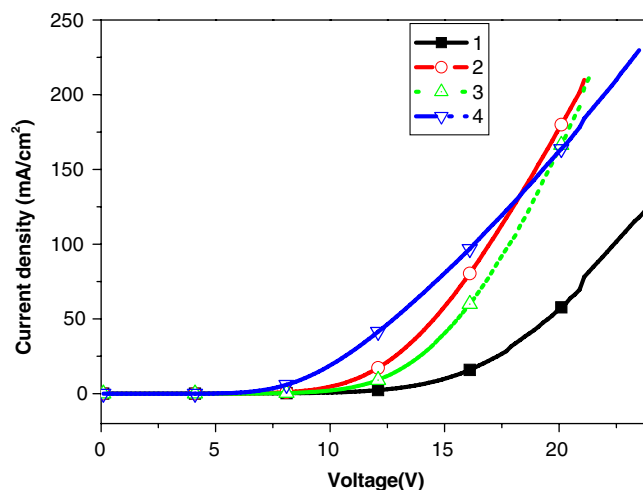


Fig. 4. Current density vs. voltage characteristics of the devices fabricated using the complexes 1–3 at 3 wt%, 4 at 5 wt% doping concentration.

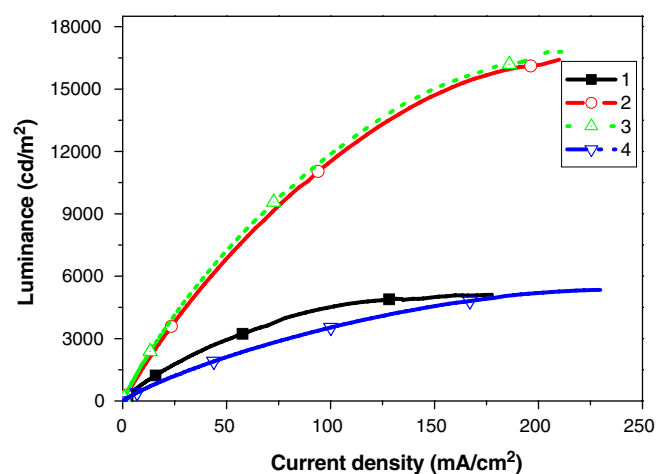


Fig. 5. Luminance vs. current density characteristics of the devices fabricated using the complexes 1–3 at 3 wt%, 4 at 5 wt% doping concentration.

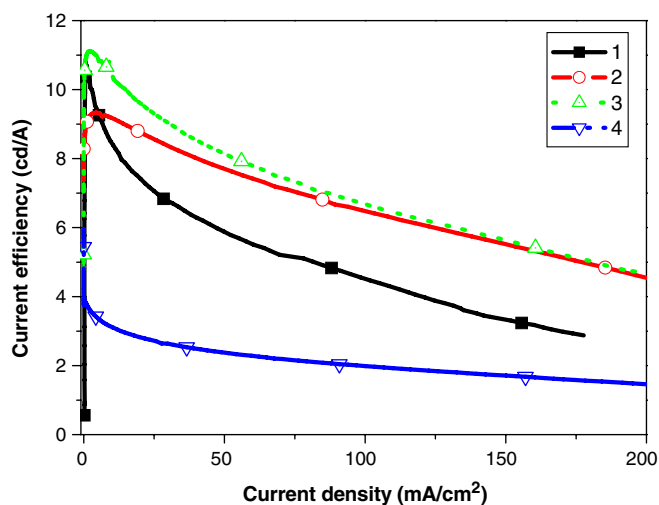


Fig. 6. Current efficiency vs. current density characteristics of the devices fabricated using the complexes 1–3 at 3 wt%, 4 at 5 wt% doping concentration.

Table 3
EL performances of devices

Complex	1				3			4
	3	3	5	8	3	5	8	5
wt% ^a								
L (cd/m) ^b	1500	3291	1088	1751	3475	1870	2284	1070
L_{\max} (cd/m ²)	5107	16410	5423	4311	16797	11477	10113	5343
η_c (cd/A) ^b	7.41	8.80	3.09	4.84	9.58	5.34	4.55	2.83
η_c (cd/A) ^c	4.47	6.50	2.12	2.39	6.64	3.94	6.33	1.99
$\eta_{c \max}$ (cd/A)	10.79	9.34	4.36	5.44	11.12	6.94	6.44	3.94
η_p (lm/W) ^b	1.39	2.25	0.74	0.89	2.23	1.76	1.32	0.88
η_p (lm/W) ^c	0.62	1.21	0.34	0.31	1.16	0.84	0.76	0.38
$\eta_{p \max}$ (lm/W)	3.40	5.20	1.37	1.21	4.97	4.72	1.54	2.87
Voltage (V) ^b	16.7	12.5	9.5	17.1	13.5	9.5	14.9	10.3
V_{ON} (V) ^d	5.7	4.5	5.0	8.2	4.5	5.1	7.3	4.3
λ_{\max} (nm)	616	605	609	611	593	596	598	605

^a Doping concentration of complex into host.

^b Recorded at 20 mA/cm².

^c Recorded at 100 mA/cm².

^d Recorded at the brightness of 1 cd/m².

density (J) for the devices is displayed in Fig. 6. The performance data of the devices are summarized in Table 3.

Comparing with using the unfluorinated complex **1** as the emitter, significantly higher performance and lower turn-on voltage were achieved when using the fluorinated complexes under the same doping level (see Figs. 4–6 and Table 3). The lower turn-on voltage is presumably due to the decreasing electron injection barrier after introduction of the fluorinated substituents, which is in agreement with the lower LUMO level estimated from the results of cyclic voltammetry (vide supra).

All the devices show a gradual decreasing in η_c with increasing current density, attributed to increasing triplet–triplet annihilation of the phosphor-bound excitons [17]. We note that the current efficiency decrease smaller extent for the fluorinated complexes than that for the unfluorinated complex **1**. For example, with the 3 wt% doping level, the current efficiency lost by 40% for **1**, 26% for **2** and 30% for **3**, respectively, when the current density changed from 20 mA/cm² to 100 mA/cm². To complex **2**, even at high current density of 100 mA/cm², L (luminance), η_c and η_p (power efficiency) still remain as high as 11774 cd/m², 6.50 cd/A and 1.12 lm/W, respectively, and to complex **3**, those data are 11995 cd/m², 6.64 cd/A and 1.16 lm/W, respectively. This phenomenon implies that the introduction of fluorinated substituent alleviates the triplet–triplet annihilation.

The dependence of EL performance on the doping concentration was studied for the devices based on the complexes **2** and **3**, under 3 wt%, 5 wt% and 8 wt% doping level in host CBP, respectively. The markedly higher luminance efficiency and brightness were achieved under the 3 wt% doping concentration for both **2** and **3** (Table 3). To complex **2**, the maximum luminance (L_{\max}) is 16410 cd/m² at a current density of 210 mA/cm². The maximum luminance efficiency ($\eta_{c \max}$) and power efficiency ($\eta_{p \max}$) are 9.34 cd/A and 5.20 lm/W, respectively. To complex **3**, those data are 16797 cd/m² at a current density of 211 mA/cm²,

11.12 cd/A and 4.97 lm/W, respectively. Neglectable redshift of EL emission peak implies the absence of aggregation or stacking up to 8% doping level. The driving voltages of these devices increase with dopant concentrations, consistent with earlier reports that iridium complexes behave as carrier traps in devices [18].

3. Conclusion

In conclusion, we have synthesized and characterized a series of novel iridium(III) complexes bearing fluorinated 2,4-diphenylquinoline ligands. Significantly mixing of the singlet and triplet excited states is clearly observed in both the absorption and emission spectra of the complexes. The emission of the complexes can be fine tuned in the orange-red region by fluorination on the ligands frame. The alteration of emission wavelength correlates with the variation of energy gap evaluated from the results of cyclic voltammetry. The effect of different *meta*-fluorine substitution on emission of cyclometalated iridium complexes is clarified. Finally, very highly efficient OLED using the complexes as the phosphorescent dopant have been demonstrated. Significantly improved performance, lower turn-on voltage and alleviated triplet–triplet annihilation were achieved using the fluorinated complexes as the emitter than that using the unfluorinated counterpart **1** under the same doping level, indicating the advantages of introduction of fluorinated substituent on the phenylquinoline ligand frame.

4. Experimental

4.1. General information

¹H NMR spectra were measured on a MECUYR-VX300 spectrometer in CDCl₃ using tetramethylsilane as an internal reference. Elemental analyses of carbon, hydrogen, and nitrogen were performed on a Carlorerba-1106

microanalyzer. Mass spectra were measured on a ZAB 3F-HF mass spectrophotometer. UV–Vis absorption spectra were recorded on Shimadzu 160A recording spectrophotometer. PL spectra were recorded on Perkin–Elmer LS 55 luminescence spectrophotometer.

Cyclic voltammetry (CV) was carried out in nitrogen-purged anhydrous THF or dichloromethane at room temperature with CHI voltammetric analyzer. Tetrabutylammonium hexafluorophosphate (TBAPF₆) (0.1 M) was used as supporting electrolyte. The conventional three-electrode configuration consists of platinum working electrode, a platinum wire auxiliary electrode, and an Ag wire pseudoreference electrode with ferrocenium/ferrocene (Fc⁺/Fc) as the internal standard. Cyclic voltammograms were obtained at scan rate of 100 mV. Formal potentials are calculated as the average of cyclic voltammetric anodic and cathodic peaks.

4.2. Preparation of ligands

6-Chloro-2-(2-fluorophenyl)-4-phenylquinoline, 6-chloro-2-(4-fluorophenyl)-4-phenylquinoline, 6-chloro-2-(4-trifluoromethyl)-4-phenylquinoline were conveniently prepared from 5-chloro-2-aminobenzophenone and corresponding acetophenone derivatives through Friedländer reaction.

5-Chloro-2-aminobenzophenone (0.93 g, 4.0 mmol) or 5-bromo-2-amino-benzophenone (1.10 g, 4.0 mmol) and 4.0 mmol acetophenone were dissolved in 15 ml of HOAc, and then 0.25 ml of concentrated H₂SO₄ was added. After refluxed for 12 h under the argon atmosphere, the solution was poured into a mixture of 50 ml of concentrated NH₃ · H₂O and 50 g of ice water. The resulting precipitate was filtered and washed with water. The pure compounds were recrystallized from THF/ethanol.

6-Bromo-2,4-diphenylquinoline: white solid, 0.93 g (65%). ¹H NMR (CDCl₃, 300 MHz) δ: 8.20 (d, *J* = 1.5 Hz, 1H), 8.17 (s, 1H), 8.11 (d, *J* = 9.0 Hz, 1H), 8.04 (d, *J* = 2.1 Hz, 1H), 7.84 (s, 1H), 7.81 (dd, *J* = 9.0, 2.1 Hz, 1H), 7.58–7.48 (m, 8H).

6-Chloro-2-(2-fluorophenyl)-4-phenylquinoline: white solid, 0.48 g (36%). M.p.: 136–139 °C. IR [cm⁻¹, KBr]: 2925(s), 1629(s), 1441(s), 1383(m), 1259(m), 1097(m). ¹H NMR (CDCl₃, 300 MHz) δ: 8.12 (m, 3H), 7.89 (d, *J* = 2.4 Hz, 1H), 7.79 (d, *J* = 2.7 Hz, 1H), 7.64 (dd, *J* = 9.0, 2.4 Hz, 1H), 7.42 (m, 1H), 7.31 (td, *J* = 7.8, 1.2 Hz, 1H), 7.21 (m, 1H).

6-Chloro-2-(4-fluorophenyl)-4-phenylquinoline: white solid, 0.66 g (49%). M.p.: 176–178 °C. IR [cm⁻¹, KBr]: 3008(s), 1706(s), 1451(s), 1380(m), 1259(m), 1070(m). ¹H NMR (CDCl₃, 300 MHz) δ: 8.08 (m, 3H), 7.77 (d, *J* = 2.4 Hz, 1H), 7.70 (s, 1H), 7.58 (dd, *J* = 8.7, 1.8 Hz, 1H), 7.47 (m, 5H), 7.12 (m, 2H).

6-Chloro-2-(4-trifluoromethyl)-4-phenylquinoline: white solid, 0.63 g (41%). M.p.: 117–119 °C. IR [cm⁻¹, KBr]: 2975(s), 1590(s), 1483(s), 1328(m), 1150(m). ¹H NMR (CDCl₃, 300 MHz) δ: 8.21 (s, 1H), 8.18 (s, 1H), 8.06 (d, *J* = 8.7 Hz, 1H), 7.78 (d, *J* = 2.1 Hz, 1H), 7.74 (s, 1H),

7.69 (s, 1H), 7.66 (s, 1H), 7.58 (dd, *J* = 8.7, 2.1 Hz, 1H), 7.46 (m, 5H).

4.3. Preparation of Ir complexes

The mixture of organic ligand (1.42 mmol), IrCl₃ · 3H₂O (0.21 g 0.59 mmol) in a mixed solvent of 2-ethoxyethanol (12 ml) and water (4 ml) was stirred under argon at 120 °C for 24 h. Cooled to room temperature, the precipitate was collected by filtration and washed with water, ethanol and hexane successively, and then dried in vacuum to give a cyclometallated Ir(III) μ-chloro-bridged dimer. The dimer (0.12 g, 0.08 mmol), acetylacetonone (0.24 mmol) and Na₂CO₃ (86 mg, 0.8 mmol) were dissolved in 2-ethoxyethanol (8 ml) and the mixture was then stirred under argon at 100 °C for 16 h. After cooling to room temperature, the precipitate was filtered off and washed with water, ethanol and hexane. The crude product was flash chromatographed on silica gel using CH₂Cl₂ as eluent to afford the desired Ir(III) complex.

Complex 1: yield: 62%. ¹H NMR (CDCl₃, 300 MHz) δ: 8.44 (d, *J* = 9.3 Hz, 2H), 8.01 (s, 2H), 7.99 (s, 2H), 7.82 (d, *J* = 7.5 Hz, 2H), 7.66–7.62 (m, 10H), 7.48 (d, *J* = 9.6 Hz, 2H), 6.85 (t, *J* = 7.5 Hz, 2H), 6.67 (d, *J* = 6.9 Hz, 2H), 6.56 (d, *J* = 7.5 Hz, 2H), 4.76 (s, 1H), 1.56 (s, 6H). Anal. Calc. for C₄₇H₃₃IrN₂O₂Br₂: C, 55.90; H, 3.29; N, 2.77. Found: C, 55.69; H, 3.41; N, 2.55%. MS (FAB): *m/z* 1010 (M⁺).

Complex 2: yield: 54%. ¹H NMR (CDCl₃, 300 MHz) δ: 8.49 (d, *J* = 3.3 Hz, 2H), 8.40 (d, *J* = 9.6 Hz, 2H), 7.82 (d, *J* = 2.4 Hz, 2H), 7.63–7.58 (m, 10H), 7.32 (dd, *J* = 9.6, 2.1 Hz, 2H), 6.64 (d, *J* = 5.2 Hz, 2H), 6.60 (s, 2H), 6.33 (m, 2H), 4.69 (s, 1H), 1.56 (s, 6H). Anal. Calc. for C₄₇H₃₁IrN₂O₂Cl₂F₂: C, 58.99; H, 3.27; N, 2.93. Found: C, 58.74; H, 3.43; N, 2.79%. MS (FAB): *m/z* 956 (M⁺).

Complex 3: yield: 58%. ¹H NMR (CDCl₃, 300 MHz) δ: 8.46 (d, *J* = 9.6 Hz, 2H), 8.20–8.16 (m, 2H), 7.94 (s, 2H), 7.83–7.79 (m, 4H), 7.66–7.55 (m, 8H), 7.38 (dd, *J* = 9.6, 1.8 Hz, 2H), 6.90 (td, *J* = 9.0, 2.4 Hz, 2H), 6.18 (dd, *J* = 9.6, 2.4 Hz, 2H), 4.79 (s, 1H), 1.59 (d, *J* = 7.8 Hz, 6H). Anal. Calc. for C₄₇H₃₁IrN₂O₂Cl₂F₂: C, 58.99; H, 3.27; N, 2.93. Found: C, 58.64; H, 3.05; N, 3.26%. MS (FAB): *m/z* 956 (M⁺).

Complex 4: yield: 60%. ¹H NMR (CDCl₃, 300 MHz) δ: 8.36 (d, *J* = 9.6 Hz, 2H), 8.07 (s, 2H), 7.93 (d, *J* = 8.1 Hz, 2H), 7.87 (d, *J* = 2.1 Hz, 2H), 7.68–7.60 (m, 10H), 7.37 (dd, *J* = 9.6, 3.0 Hz, 2H), 7.22 (s, 2H), 6.79 (s, 2H), 4.73 (s, 1H), 1.55 (s, 6H). Anal. Calc. for C₄₉H₃₁IrN₂O₂Cl₂F₆: C, 55.68; H, 2.96; N, 2.65. Found: C, 55.74; H, 2.99; N, 2.93%. MS (FAB): *m/z* 1056 (M⁺).

4.4. OLED fabrication

Organic layers and metal cathode were fabricated by high-vacuum thermal evaporation onto a pre-cleaned indium tin oxide (ITO) glass substrate. In a vacuum chamber with a pressure of <10⁻⁴ Pa, 40 nm of NPD as the hole

transporting layer, 30 nm of the complex doped (10%) CBP as the emitting layer, 10 nm of BCP as a hole and exciton blocking layer, 30 nm of AlQ₃ as the electron transporting layer, and a cathode composed of 1 nm of lithium fluoride and 100 nm of aluminum were sequentially deposited onto the substrate to construct the device. The *I–V–B* of EL devices was measured at ambient condition with a Keithley 2400 Source meter and a Keithley 2000 Source multimeter equipped with a calibrated silicon photodiode. The EL spectra were measured by JY SPEX CCD3000 spectrometer.

Acknowledgments

We thank the National Natural Science Foundation of China (Project Nos. 20371036 and 20474047), the Program for New Century Excellent Talents in University, the Scientific Research Foundation for Returned Overseas Chinese Scholars, the Ministry of Education of China, for financial support.

References

- [1] For example: (a) M.A. Baldo, S. Lamansky, P.E. Burrows, M.E. Thompson, S.R. Forrest, *Appl. Phys. Lett.* 75 (1999) 4; (b) C. Adachi, M.A. Baldo, S.R. Forrest, M.E. Thompson, *Appl. Phys. Lett.* 77 (2000) 904; (c) S. Lamansky, P. Djurovich, D. Murphy, F. Abdel-Razzaq, R. Kwong, I. Tsyba, M. Bortz, B. Mui, R. Bau, M.E. Thompson, *Inorg. Chem.* 40 (2001) 1704; (d) S. Lamansky, P. Djurovich, D. Murphy, F. Abdel-Razzaq, H.E. Lee, C. Adachi, P.E. Butto, S.R. Forrest, M.E. Thompson, *J. Am. Chem. Soc.* 123 (2001) 4304; (e) M.K. Nazeeruddin, R. Humphry-Baker, D. Berner, S. Rivier, L. Zuppiroli, M. Graetzel, *J. Am. Chem. Soc.* 125 (2003) 8790; (f) A.B. Tamayo, B.D. Alleyne, P.I. Djurovich, S. Lamansky, I. Tsyba, N.N. Ho, R. Bau, M.E. Thompson, *J. Am. Chem. Soc.* 125 (2003) 7377; (g) A. Tsuboyama, H. Iwakaki, M. Furugori, T. Mukaide, J. Kamatani, S. Igawa, T. Moriyama, S. Miura, T. Takiguchi, S. Okada, M. Hoshino, K. Ueno, *J. Am. Chem. Soc.* 125 (2003) 12971; (h) J. Kim, I.S. Shin, H. Kim, J.K. Lee, *J. Am. Chem. Soc.* 127 (2005) 1614; (i) X. Zhang, Z. Chen, C. Yang, Z. Li, K. Zhang, H. Yao, J. Qin, J. Chen, Y. Cao, *Chem. Phys. Lett.* 422 (2006) 386.
- [2] (a) C.H. Yang, C. Tai, I.W. Sun, *J. Mater. Chem.* 14 (2004) 947; (b) J.P. Duan, P.P. Sun, C.H. Cheng, *Adv. Mater.* 15 (2003) 224; (c) Y.J. Su, H.L. Huang, C.L. Li, C.H. Chien, Y.T. Tao, P.T. Chou, S. Datta, R.S. Liu, *Adv. Mater.* 15 (2003) 884.
- [3] (a) W.C. Chien, A.T. Hu, J.P. Duan, D.K. Raybarapu, C.H. Chien, *J. Organomet. Chem.* 689 (2004) 4882; (b) I.R. Laskar, T.M. Chen, *Chem. Mater.* 16 (2004) 111.
- [4] (a) W.S. Huang, J.T. Lin, C.H. Chien, Y.T. Tao, S.S. Sun, Y.S. Wen, *Chem. Mater.* 16 (2004) 2480; (b) L. Chen, C. Yang, J. Qin, J. Gao, H. You, D. Ma, *J. Organomet. Chem.* 691 (2006) 3519.
- [5] (a) R.A. Negres, X. Gong, J.C. Ostrowski, G.C. Bazan, D. Moses, A.J. Heeger, *Phys. Rev. B* 68 (2003) 115209; (b) X. Gong, J.C. Ostrowski, D. Moses, G.C. Bazan, A.J. Heeger, *Adv. Funct. Mater.* 13 (2003) 439; (c) P.A. Lane, L.C. Palilis, D.F. O'Brien, C. Giebeler, A.J. Cadby, D.G. Lidzey, A.J. Campbell, W. Blau, D.D.C. Bradley, *Phys. Rev. B* 63 (2001) 235206.
- [6] (a) F.I. Wu, H.J. Su, C.F. Shu, L. Luo, W.G. Diao, C.H. Cheng, J.P. Duan, G.H. Lee, *J. Mater. Chem.* 15 (2005) 1035; (b) H.C. Li, P.T. Chou, Y.H. Hu, Y.M. Cheng, R.S. Liu, *Organometallics* 24 (2005) 1329; (c) K.R.J. Thomas, M. Velusamy, J.T. Lin, C.H. Chien, Y.T. Tao, Y.S. Wen, Y.H. Hu, P.T. Chou, *Inorg. Chem.* 44 (2005) 5677; (d) C.Y. Jiang, W. Yang, J.B. Peng, S. Xiao, Y. Cao, *Adv. Mater.* 16 (2004) 537.
- [7] (a) V.V. Grushin, N. Herron, D.D. LeCloux, W.J. Marshall, V.A. Petrov, Y. Wang, *Chem. Commun.* (2001) 1494; (b) Y. Wang, N. Herron, V.V. Grushin, D. LeCloux, V.A. Petrov, *Appl. Phys. Lett.* 79 (2001) 449.
- [8] (a) M.R. Robinson, M.B. O'Regan, G.C. Bazan, *Chem. Commun.* (2000) 1645; (b) J.C. Ostrowski, M.R. Robinson, A.J. Heeger, G.C. Bazan, *Chem. Commun.* (2002) 784.
- [9] P.D. Sybert, W.H. Beever, J.K. Stille, *Macromolecules* 14 (1981) 493.
- [10] M. Nonoyama, *Bull. Chem. Soc. Jpn.* 47 (1974) 767.
- [11] (a) K.A. King, P.J. Spellane, R.J. Watts, *J. Am. Chem. Soc.* 107 (1985) 1431; (b) S. Sprouse, K.A. King, P.J. Spellane, R.J. Watts, *J. Am. Chem. Soc.* 106 (1984) 6647; (c) K.A. King, R.J. Watts, *J. Am. Chem. Soc.* 109 (1987) 1589.
- [12] (a) P.J. Hay, *J. Phys. Chem. A* 106 (2002) 1634; (b) J. Brooks, Y. Babayan, S. Lamansky, P.I. Djurovich, M.E. Thompson, *Inorg. Chem.* 41 (2002) 3055.
- [13] J. Pommerehne, H. Vestweber, W. Guss, R.F. Mahrt, H. Bassler, M. Porsch, J. Daub, *Adv. Mater.* 7 (1995) 551.
- [14] J. Li, P.I. Djurovich, B.D. Alleyne, M. Yousufuddin, N.N. Ho, J.C. Thomas, J.C. Peters, R. Bau, M.E. Thompson, *Inorg. Chem.* 44 (2005) 1713.
- [15] (a) P. Coppo, E.A. Plummer, L.D. Cola, *Chem. Commun.* (2004) 1774; (b) S. Takizawa, J. Nishida, T. Tsuzuki, S. Tokito, Y. Yamashita, *Chem. Lett.* 34 (2005) 1222; (c) K. Dedeian, J. Shi, N. Shepherd, E. Forsythe, D.C. Morton, *Inorg. Chem.* 44 (2005) 4445.
- [16] (a) Q. Zhang, Q. Zhou, Y. Cheng, L. Wang, D. Ma, X. Jing, *Adv. Mater.* 16 (2004) 432; (b) L. Chen, C. Yang, J. Qin, J. Gao, D. Ma, *Synth. Met.* 152 (2005) 225.
- [17] M.A. Baldo, C. Adachi, S.R. Forrest, *Phys. Rev. B* 62 (2000) 10967.
- [18] (a) X. Ren, B.D. Alleyne, P.I. Djurovich, C. Adachi, I. Tsyba, R. Bau, M.E. Thompson, *Inorg. Chem.* 43 (2004) 1697; (b) B.W. D'Andrade, S. Datta, S.R. Forrest, P. Djurovich, E. Polikarpov, M.E. Thompson, *Org. Electron.* 6 (2005) 11.